Supplement of Atmos. Chem. Phys., 25, 15415–15435, 2025 https://doi.org/10.5194/acp-25-15415-2025-supplement © Author(s) 2025. CC BY 4.0 License.





Supplement of

Variability in BVOC emissions and air quality impacts among urban trees in Montreal and Helsinki

Kaisa Rissanen et al.

Correspondence to: Kaisa Rissanen (kaisa.rissanen@helsinki.fi)

The copyright of individual parts of the supplement might differ from the article licence.

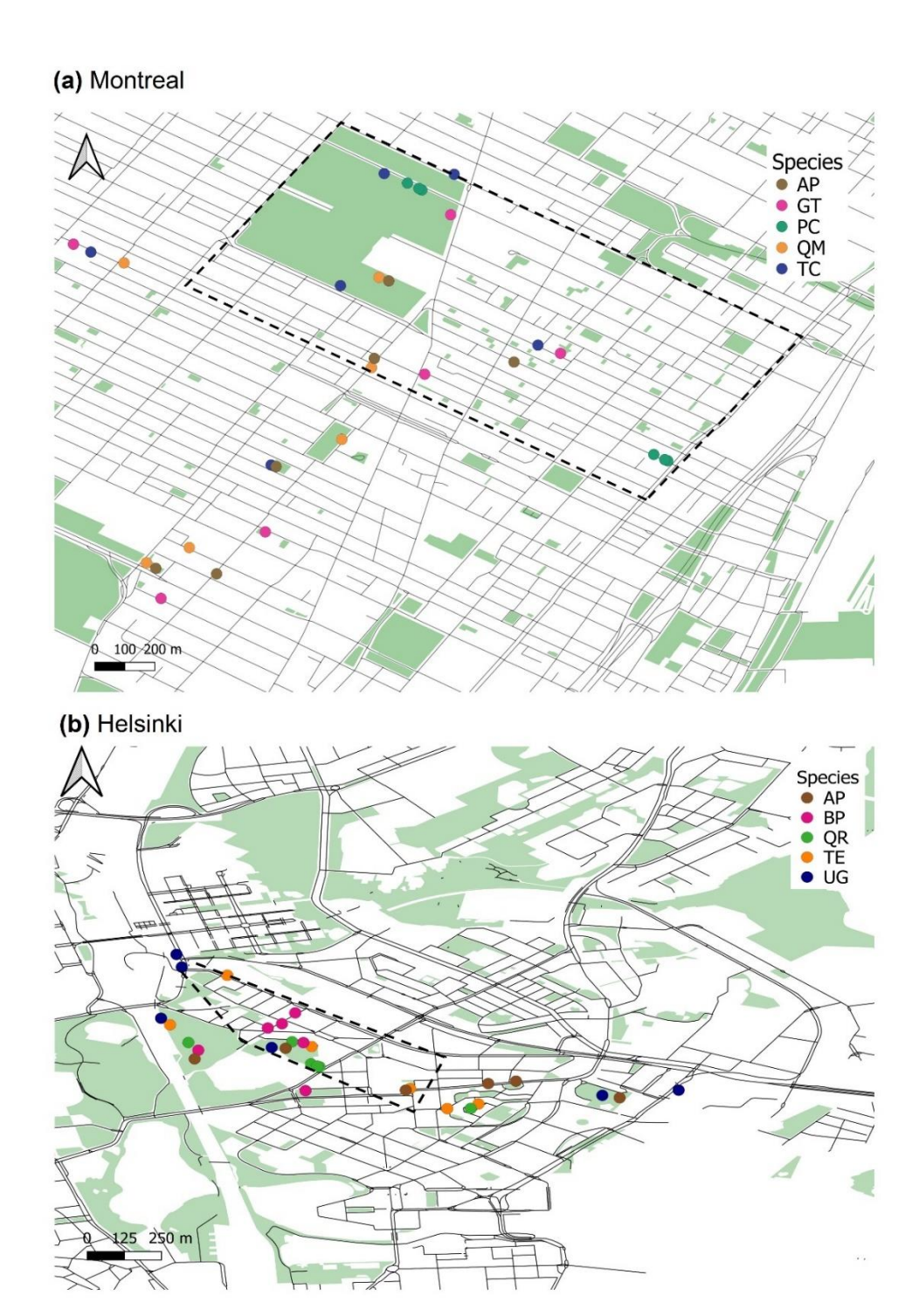


Figure S1. Maps indicating the locations of the study trees in (a) Montreal and (b) Helsinki. The dashed lines outline the upscaling test areas for the upscaling BVOC emissions and ozone and secondary organic aerosol formation by study species. AP, *Acer platanoides*; GT, *Gleditsia triacanthos*; PC, *Populus canescens*; QM, *Quercus macrocarpa*; TC, *Tilia cordata*; BP, *Betula pendula*; QR, *Quercus robur*; TE, *Tilia x europaea*; UG, *Ulmus glabra*.

Table S1. The measurement date, ambient environmental conditions during measurements between 11.00 and 15.00 (T, temperature; RH, relative humidity), and the number, species, and site types of the sampled trees per day. For ambient temperatures and precipitation totals for the full months, see Fig. S4. AP, *Acer platanoides*; GT, *Gleditsia triacanthos*; PC, *Populus canescens*; QM, *Quercus macrocarpa*; TC, *Tilia cordata*; BP, *Betula pendula*; QR, *Quercus robur*; TE, *Tilia x europaea*; UG, *Ulmus glabra*.

	Ambient conditions		Sampled trees			
Dates	T (°C)	RH (%)	n	street trees	park trees	
Montreal						
2 June	22-29	41-52	3	GT	AP, QM	
3 June	26-32	31-33	3	TC, AP	GT	
4 June	26-33	26–36	3	OM AD	AP, TC, QM	
7 June	28-31	30-33	3	QM, AP, GT	QM, AP,	
8 June	19-23	53-56	3		TC	
10 June	22-23	47-50	3	TC, AP	GT	
11 June	27-33	24-32	3	PC, PC, PC		
13 June	24—27	37–41	3	TC GT, TC,	GT, PC	
14 June	28-33	29-33	3	QM		
15 June	26	45–47	3		PC, PC, TC	
11 Aug	31-34	38-44	3	AP	AP, QM	
13 Aug	26–27	32-41	3	TC, AP	GT AP, TC,	
15 Aug	27-30	22-43	3	AP, QM,	QM	
16 Aug	27-33	37–47	3	GT	AD OM	
17 Aug	24-30	45-55	3		AP, QM, TC	
19 Aug	23-35	35-57	3	QM, AP	GT	
20 Aug	30-37	27-40	3	PC, PC, PC		
22 Aug	28-30	50-58	3	TC	GT, PC	
24 Aug	28-31	46-54	3	TC, GT, QM		
25 Aug	21—25	43—55	3		PC, PC, TC	
<u>Helsinki</u>						
6 July 7 July	22-25	42—47	2	TE, UG,	AP, UG	
	25-31	34-47	3	UG		
8 July	28-31	25-29	3		QR, TE, BP	
11 July	26-28	37-43	3	AP	TE, QR	
12 July	22-24	58-62	3	BP	BP, AP	
14 July	22-30	37-57	3	TE, TE, AP		
19 July	22-31	37-56	2	UG, AP		
20 July	24-30	27-37	3	QR	UG, AP	
21 July	29-30	33-36	3		QR, TE, UG	
22 July	26-33	37–49	3	QR, QR	BP	
25 July	25-29	31–42	2	BP, BP		

S1. LOOK oven bag retention tests

We tested the pretreated polyethylene terephthalate (PET) (LOOK oven bag 45 x 55 cm) bags to ensure acceptable blanks and yields for the compounds studied. We first attached the bags to a polytetrafluoroethylene (PTFE) backplate and used a ¼-in fluorinated ethylene propylene (FEP) tube connected through it to push air in and pull samples out. The connection to the bag and backplate was not fully airtight, so we employed a slight overpressure to ensure that no outside contaminants would enter. Just outside the PTFE backplate, silcosteel t-cross unions in the ¼-in FEP tubes allowed for Tenax-TA & Carbopack B absorbent tube sampling. We performed the tests by introducing clean air or a gas mixture with known compounds to the bag and measuring the concentration of the air entering and exiting the bag. A commercial zero-air generator (HPZA-7000, Parker Hannifin Corporation) produced the clean air flow. After the zero-air generator, a bubbler humidified the air flow to ensure that the air was not completely dry, because this is not normal in field measurements. We produced the gas mixture by continually injecting a methanol solution including the studied compounds (Table S2) into the clean air flow using an automated syringe. To maximise the potential wall losses on the bag surfaces, we guided the incoming air to the back of the bag via tubing and collected the outgoing air near the mouth of the back. We repeated the test three times and calculated the average yield. The injection and flow consistencies caused some uncertainties, whereby we normalised the results using toluene, given its expectation to perform well.

Table S2. The tested compounds, average yield (%), and standard deviation (SD) of yield for a pretreated LOOK oven bag.

Tested compound in the gas mixture	Average yield (%)	SD
Methacrolein	117	32
MBO	91	7.2
cis-3-Hexenol	92	8.0
α-pinene	99	0.7
Camphene	99	0.2
β-pinene	98	1.8
Δ^3 -carene	99	1.8
ρ-cymene	99	1.3
Limonene	99	1.6
1,8-cineol	98	6.1
Terpinolene	97	6.0
Linalool	88	5.0
4-acetyl-1-methylcyclohexene	92	4.2
Nopinone	92	4.1
Longicyclene	97	3.5
Iso-longifolene	96	6.2
β -farnesene	93	7.5
β-caryophyllene	80	4.6
α-humulene	92	6.9
Caryophyllene oxide	22	22



Figure S2. The measurement system: FEP tubing, PET bag, T and RH sensor (inside the bag), and PAR sensor (on top of the wooden support) attached to a *Betula pendula* branch in Helsinki in July 2022.

Table S3. List of detected and calibrated compounds with the ranges of analytical and measurement system detection limits (ng per tube, as mean + 3 SDs). Compounds were in the calibration standard (*) or calibrated as another compound in the calibration standard.

	Calibrated (*) or	Analytical detection	Sampling system detection limit
Compound	analysed as	limit (ng per tube)	(ng per tube)
Hemiterpenes			
isoprene	*	0.200-41.41	0.258-1.589
methacrolein	*	0.279-2.182	0.252-0.565
Monoterpenoids			
1,8-cineol	*	0.023-0.362	0.009-0.019
α-pinene	*	0.006-0.196	0.017-0.039
β-pinene	*	0.007-0.446	0.014-0.167
camphene	*	0.017-0.122	0.006-0.017
Δ^3 -carene	*	0.008-0.041	0.017-0.023
limonene	*	0.013-0.654	0.035-0.082
linalool	*	0.057-0.161	0.034-0.222
myrcene	as β-pinene	0.009-0.567	0.010-0.050
nopinone	*	0.038-0.417	0.035-0.054
ρ-cymene	*	0.016-0.292	0.006-0.032
sabinene	as β-pinene	0.007-0.283	0.012-0.180
terpinolene	*	0.032-0.165	0.044-0.132
monoterpenoid 1	as α-pinene	0.008-0.304	0.005-0.013
monoterpenoid 2	as β-pinene	0.004-0.161	0.005-0.013
monoterpenoid 3	as Δ^3 -carene	0.004-0.031	0.004-0.016
monoterpenoid 4	as 1,8-cineole	0.004-0.059	0.009-0.019
monoterpenoid 5	as terpinolene	0.008-0.539	0.012-0.022
monoterpenoid 6	as terpinolene	0.009-0.156	0.009-0.189
monoterpenoid 7	as terpinolene	0.005-0.586	0.056-0.089
monoterpenoid 8	as linalool	0.010-0.043	0.006-0.014
monoterpenoid 9	as nopinone	0.010-0.121	0.026-0.038
monoterpenoid 10	as nopinone	0.021-0.065	0.034-0.038
monoterpenoid 11	as carene	0.003-0.023	0.000-0.007
monoterpenoid 12	as linalool	0.011-0.037	0.007-0.018
monoterpenoid 13	as linalool	0.012-0.034	0.007-0.015
monoterpenoid 14	as nopinone	0.056-0.608	0.051-0.129
monoterpenoid 15	as nopinone	0.037-0.680	0.034-0.076
monoterpenoid 16	as nopinone	0.095-0.882	0.056-0.219
monoterpenoid 17	as nopinone	0.068-0.440	0.064-0.134
monoterpenoid 18	as nopinone	0.061-0.307	0.044-0.101
monoterpenoid 19	as nopinone	0.028-0.952	0.081-0.423
Sesquiterpenoids			
α-farnesene	as α-humulene	0.005-0.028	0.004-0.010
α-humulene	*	0.062-0.391	0.010-0.014
β-caryophyllene	*	0.084-0.373	0.019-0.040
β-farnesene	*	0.244-2.626	0.081-0.285
caryophyllene oxide	*	0.231-1.016	0.169-0.228
iso-longifolene	*	0.044-0.464	0.005-0.010
longicyclene	*	0.047-0.357	0.006-0.015
sesquiterpenoid 1	as iso-longifolene	0.005-0.060	0.005-0.006

	î.	i	
sesquiterpenoid 2	as iso-longifolene	0.004-0.101	0.004-0.031
sesquiterpenoid 4	as iso-longifolene	0.012-0.057	0.007-0.010
sesquiterpenoid 5	as β-caryophyllene	0.025-0.127	0.011-0.067
sesquiterpenoid 7	as α-humulene	0.018-0.043	0.017-0.023
sesquiterpenoid 8	as α-humulene	0.007-0.104	0.006-0.012
sesquiterpenoid 9	as α-humulene	0.010-1.392	0.007-0.010
sesquiterpenoid 10	as α-humulene	0.005-0.595	0.009-0.077
sesquiterpenoid 11	as α-humulene	0.006-0.020	0.002-0.006
GLVs			
cis-3-hexenol	*	0.079-0.503	0.037-0.066
trans-3-hexenol	as cis-3-hexenol	0.072-0.366	0.018-0.128
hexenyl acetate	as Δ^3 -carene	0.005-0.012	0.007-0.015
MBO	*	0.008-0.047	0.006-0.031
GLV 1	as cis-3-hexenol	0.0370.098	0.038-0.583
	1		
GLV 2	as cis-3-hexenol	0.056-0.646	0.087 - 0.582

S2. Correction for BVOC loss due to ozone reactivity

To estimate any loss due to the ozone reactivity of compounds, we used the slopes for terpenoid losses as quantified by Helin et al. (2020). For the purge volume, we used the air volume sampled in the tube, relative to the ratio of our measured O₃ concentration (from 10 to 42 ppb) and an O₃ concentration of 40 ppb, previously used by Helin et al. (2020).

For those compounds not included in Helin et al.'s (2020) study, we estimated the slope accordingly. We first fitted a linear regression between the terpenoid loss slope and their rate coefficient with O_3 (cm³ molecule⁻¹ s⁻¹) for compounds included in the Helin et al. (2020) study ($R^2 = 0.74$). We then used this regression to calculate the terpenoid loss slope based on the rate coefficients available in the literature (Atkinson et al., 1982; Fantechi et al., 1998; Neeb et al., 1998; Karl et al., 2004; Sarang et al., 2021). For unidentified monoterpenes and sesquiterpenes, we used the compound group mean slopes.

Overall, when comparing the mean values between measurements taken on days with a scrubber and without a scrubber on consecutive measurement weeks, the negative effect of the missing O_3 scrubber on the BVOC concentrations in the adsorbent tube collection incoming ambient air was small (Fig. S3). Similarly, the effect of the correction using the terpenoid loss slope was small even for compounds with some of the largest reactivities to O_3 among the compounds we studied (terpinolene, Fig. S3). The mean (SD) concentration for α -pinene with a scrubber was 0.020~(0.007), for α -pinene without a scrubber 0.013~(0.008) and 0.013~(0.008) ng L⁻¹ without a scrubber and with correction. The mean (SD) concentration for terpinolene with scrubber was 0.091~(0.031), for terpinolene without scrubber 0.114~(0.041) and without scrubber and with correction 0.118~(0.043) ng L⁻¹. In comparison, the concentrations for outgoing sample air for tubes 20–33 were on average (SD) 0.102~(0.059) ng L⁻¹ for terpinolene and 0.177~(0.259) ng L⁻¹ for α -pinene.

Helin, A., Hakola, H., Hellén, H., 2020. Optimisation of a thermal desorption--gas chromatography--mass spectrometry method for the analysis of monoterpenes, sesquiterpenes and diterpenes. Atmos. Meas. Tech. 13, 3543–3560. https://doi.org/10.5194/amt-13-3543-2020

Atkinson R, Winer AM, Pitts JN (1982) Rate constants for the gas phase reactions of O3 with the natural hydrocarbons isoprene and α - and β -pinene. Atmos Environ 16:1017–1020. https://www.sciencedirect.com/science/article/pii/0004698182901871

Fantechi G, Jensen NR, Hjorth J, Peeters J (1998) Mechanistic studies of the atmospheric oxidation of methyl butenol by OH radicals, ozone and NO3 radicals. Atmos Environ 32:3547–3556. https://www.sciencedirect.com/science/article/pii/S1352231098000612

Karl M, Brauers T, Dorn H-P, Holland F, Komenda M, Poppe D, Rohrer F, Rupp L, Schaub A, Wahner A (2004) Kinetic Study of the OH-isoprene and O3-isoprene reaction in the atmosphere simulation chamber, SAPHIR. Geophys Res Lett 31. https://doi.org/10.1029/2003GL019189

Neeb P, Kolloff A, Koch S, Moortgat GK (1998) Rate constants for the reactions of methylvinyl ketone, methacrolein, methacrylic acid, and acrylic acid with ozone. Int J Chem Kinet 30:769–776. https://doi.org/10.1002/(SICI)1097-4601(1998)30:10%3C769::AID-KIN9%3E3.0.CO

Sarang K, Rudziński KJ, Szmigielski R (2021) Green Leaf Volatiles in the Atmosphere—Properties, Transformation, and Significance. Atmosphere (Basel) 12

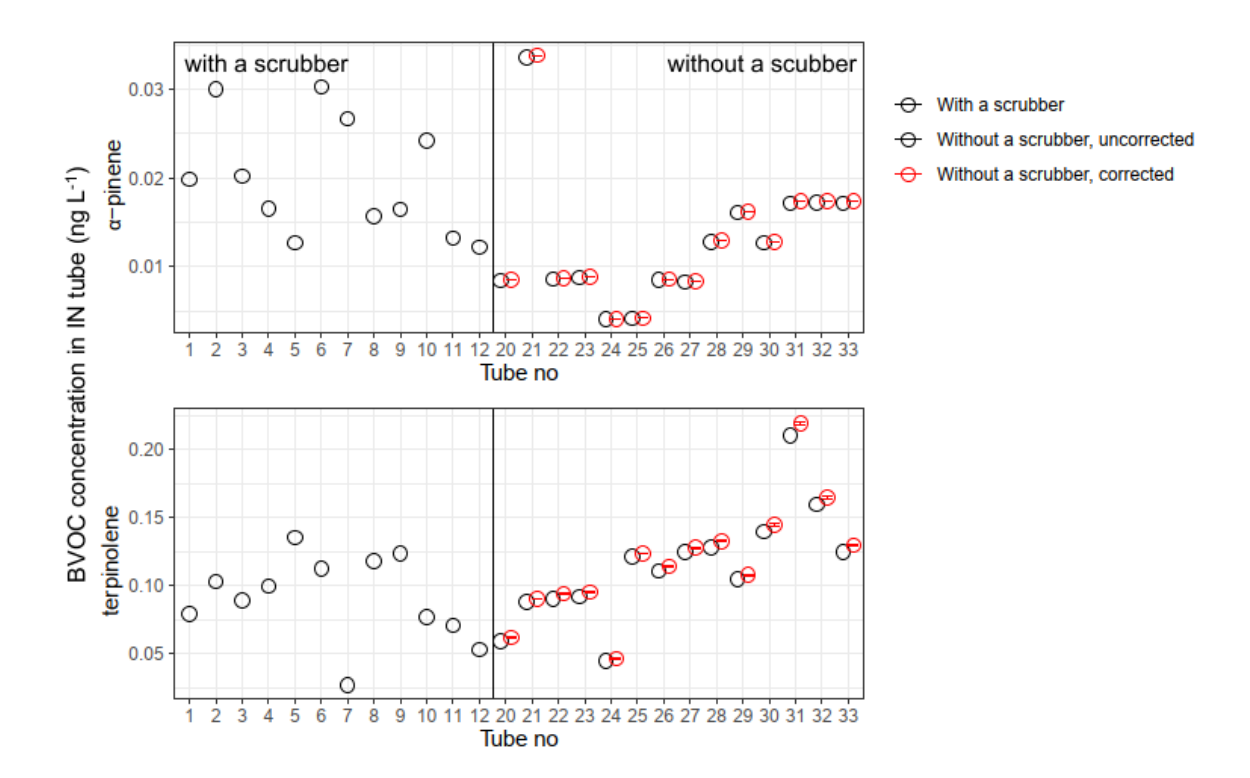


Figure S3. The adsorbent tube concentrations of α -pinene and terpinolene (as example compounds) for incoming ambient air, for sampling times with an O_3 scrubber in line before the adsorbent tube (tubes 1–12) and for sampling times without an O_3 scrubber either without (black) or with a correction (red, tubes 20–33). For a correction, the horizontal lines yield the correction using the minimal and maximal uncertainty range for the terpenoid loss slope as in Helin et al. (2020).

Table S4. The emission potentials for isoprene, monoterpenoids, and sesquiterpenoids (E, μ g g(DW)⁻¹ h⁻¹ at 30°C and 1000 μ mol m⁻² s⁻¹ photosynthetically active radiation) for the study species collected from the BVOC emission databases. When the same value is repeated in more than one database, only one reference is listed. The emission potential estimates marked with * represent genus-level estimates. The mean values are listed in Tables 3 and 4. AP, *Acer platanoides*; GT, *Gleditsia triacanthos*; PC, *Populus canescens*; QM, *Quercus macrocarpa*; TC, *Tilia cordata*; BP, *Betula pendula*; QR, *Quercus robur*; TE, *Tilia x europaea*; UG, *Ulmus glabra*.

Isoprene		Monoterp	Monoterpenoid total		
Species	${f E}$	Reference	Species	${f E}$	Reference
AP	0.02	Kaser et al., 2022	AP	1.83	Kaser et al., 2022
	0.04	Kesselmeier and Staudt, 1999		1.816*	Nowak et al., 2002
	0.114*	Nowak et al., 2002		1.5	Oderbolz et al., 2013
	0.1	Oderbolz et al., 2013	BP	3	Karl et al., 2009
BP	0	Kesselmeier and Staudt, 1999		2.8	Kaser et al., 20022
	0.05	Kaser et al., 2022		0.19	Kesselmeier and Staudt, 1999
	0.114*	Nowak et al., 2002		5.4	Kesselmeier and Staudt, 1999
GT	0.1	Kaser et al., 2022		0.227*	Nowak et al., 2002
	0.114*	Nowak et al., 2002		2.63	Owen et al., 2003
PC	79.45	Nowak et al., 2002	GT	0.7	Kaser et al., 2022
	70	Steinbecher et al., 2009		0.227*	Nowak et al., 2002
QM	79.45*	Nowak et al., 2002	PC	0.1135*	Nowak et al., 2002
	69*	Stewart et al., 2003		0	Oderbolz et al., 2013
QR	76.6	Benjamin et al., 1996		0.1*	Stewart et al., 2003
	38.45	Kaser et al., 2022	QM	0.227*	Nowak et al., 2002
	79.45*	Nowak et al., 2002		0.15*	Stewart et al., 2003
	70	Steinbecher et al., 2009	QR	0.6	Benjamin et al., 1996
	58.3*	Stewart et al., 2003		0.94	Kaser et al., 2022
TC	0*	Nowak et al., 2002		0.227*	Nowak et al., 2002
	5.5*	Owen et al., 2003		1	Steinbecher et al., 2009
TE	0*	Nowak et al., 2002		1.75	Stewart et al., 2003
	5.5*	Owen et al., 2003	TC	0*	Owen et al., 2003
UG	0.114*	Nowak et al., 2002	TE	0*	Owen et al., 2003
			UG	0.1	Benjamin et al., 1996
Sesquiterpeno	id total			0.1135*	Nowak et al., 2002
Species	E	Reference			
AP	0.1	Karl et al., 2009			
BP	2	Karl et al., 2009			
GT	0.025	Kaser et al., 2022			
PC	0.1	Karl et al., 2009			
QM	(0.1)	(no reference, taken as QR)			
QR	0.1	Karl et al., 2009			
TC	0.1	Karl et al., 2009			
TE	(0.1)	(no reference, taken as TC)			
UG	0.1	Karl et al., 2009			

References:

Benjamin, M.T., Sudol, M., Bloch, L., Winer, A.M., 1996. Low-emitting urban forests: A taxonomic methodology for assigning isoprene and monoterpene emission rates. Atmos. Environ. 30, 1437–1452. https://doi.org/10.1016/1352-2310(95)00439-4

Karl, M., Guenther, A., Köble, R., Leip, A., Seufert, G., 2009. A new European plant-specific emission inventory of biogenic volatile organic compounds for use in atmospheric transport models. Biogeosciences 6, 1059–1087. https://doi.org/10.5194/bg-6-1059-2009

Kaser, L., Peron, A., Graus, M., Striednig, M., Wohlfahrt, G., Jurán, S., Karl, T. 2022. Interannual variability of terpenoid emissions in an alpine city. Atmos. Chem. Phys. 22, 5603–5618. https://doi.org/10.5194/acp-22-5603-2022

Kesselmeier, J., Staudt, M., 1999. Biogenic volatile organic compounds (VOC): An overview on emission, physiology and ecology. J. Atmos. Chem. https://doi.org/10.1023/A:1006127516791

Nowak, D.J., Crane, D.E., Stevens, J.C., Ibarra, M. 2002. Brooklyn's urban forest. General Technical Report. NE-290. Newtown Square, PA: U. S. Department of Agriculture, Forest Service, Northeastern Forest Experiment Station 107 p. https://doi.org/10.2737/NE-GTR-290

Oderbolz, D.C., Aksoyoglu, S., Keller, J., Barmpadimos, I., Steinbrecher, R., Skjøth, C.A., Plaß-Dülmer, C., Prévôt, A.S.H., 2013. A comprehensive emission inventory of biogenic volatile organic compounds in Europe: Improved seasonality and land-cover. Atmos. Chem. Phys. 13, 1689–1712. https://doi.org/10.5194/acp-13-1689-2013

Owen, S.M., MacKenzie, A.R., Stewart, H., Donovan, R., Hewitt, C.N., 2003. Biogenic volatile organic compound (VOC) emission estimates from an urban tree canopy. Ecol. Appl. 13, 927–938. https://doi.org/10.1890/01-5177

Steinbrecher, R., Smiatek, G., Köble, R., Seufert, G., Theloke, J., Hauff, K., Ciccioli, P., Vautard, R., Curci, G., 2009. Intra- and inter-annual variability of VOC emissions from natural and semi-natural vegetation in Europe and neighbouring countries. Atmos. Environ. 43, 1380–1391. https://doi.org/10.1016/j.atmosenv.2008.09.072

Stewart, H.E., Hewitt, C.N., Bunce, R.G.H., Steinbrecher, R., Smiatek, G., Schoenemeyer, T., 2003. A highly spatially and temporally resolved inventory for biogenic isoprene and monoterpene emissions: Model description and application to Great Britain. J. Geophys. Res. Atmos. 108. https://doi.org/10.1029/2002JD002694

Table S5: Compound-wise maximum incremental reactivity (MIR) used to calculate the O3 formation potential based on Carter et al. (2010) and for the sesquiterpenoids, based on Wang et al. (2013) and Yang et al. (2023). Compound-wise fractional aerosol coefficient, (FAC) used to calculate SOA formation potential based on Grosjean et al. (1992),^a Hoffmann et al. (1997),^b Griffin et al. (1999),^c and Carlton et al. (2009).^d When several sources are mentioned, the value listed is a mean across the values provided in the sources. When no compound-specific value was available, compound group means were used, or, for sesquiterpene MIR, we used the value for C15 alkenes (1.71).

Monoterpenoids	MIR	FAC	Isoprene	MIR	FAC
α-pinene	4.51	9.37^{b}		10.61	2^{d}
camphene	4.51	13.22			
myrcene	4.04	11.8°			
β-pinene	3.52	18.83 ^{ac}	Sesquiterpenoids	MIR	FAC
carene	3.24	14.71 ^{bc}	longicyclene	1.71	64.03
ρ-cymene	4.44	13.22	iso-longifolene	1.71	64.03
limonene	4.55	30.87^{bc}	β-caryophyllene	1.71	64.47 ^{bc}
1,8-cineol	4.04	13.22	β-farnesene	1.71	64.03
terpinolene	6.36	2.88^{c}	α-humulene	1.71	63.6°
linalool	5.43	7.16^{bc}	caryophyllene oxide	1.71	64.03
nopinone	4.04	13.22	sesquiterpenoid 1	1.71	64.03
bornyl acetate	4.04	13.22	sesquiterpenoid 2	1.71	64.03
sabinene	4.19	10.19°	sesquiterpenoid 4	1.71	64.03
monoterpenoid 1	4.04	13.22	sesquiterpenoid 5	1.71	64.03
monoterpenoid 2	4.04	13.22	sesquiterpenoid 7	1.71	64.03
monoterpenoid 3	4.04	13.22	sesquiterpenoid 8	1.71	64.03
monoterpenoid 4	4.04	13.22	α-farnesene	1.71	64.03
monoterpenoid 5	4.04	13.22	sesquiterpenoid 9	1.71	64.03
monoterpenoid 6	4.04	13.22	sesquiterpenoid 10	1.71	64.03
monoterpenoid 7	4.04	13.22	sesquiterpenoid 11	1.71	64.03
monoterpenoid 8	4.04	13.22			
monoterpenoid 9	4.04	13.22			
monoterpenoid 10	4.04	13.22			
monoterpenoid 11	4.04	13.22			
monoterpenoid 12	4.04	13.22			
monoterpenoid 13	4.04	13.22			
monoterpenoid 14	4.04	13.22			
monoterpenoid 15	4.04	13.22			
monoterpenoid 16	4.04	13.22			
monoterpenoid 17	4.04	13.22			
monoterpenoid 18	4.04	13.22			
monoterpenoid 19	4.04	13.22			

References

Carlton, A.G., Wiedinmyer, C., Kroll, J.H., 2009. A review of Secondary Organic Aerosol (SOA) formation from isoprene. Atmos. Chem. Phys. 9, 4987–5005. https://doi.org/10.5194/acp-9-4987-2009

Carter, W., 2010. Updated maximum incremental reactivity scale and hydrocarbon bin reactivities for regulatory applications. Calif. Air Resour. Board Contract 1, 7–339.

Griffin, R.J., Cocker III, D.R., Flagan, R.C., Seinfeld, J.H., 1999. Organic aerosol formation from the oxidation of biogenic hydrocarbons. J. Geophys. Res. Atmos. 104, 3555–3567. https://doi.org/10.1029/1998JD100049

Grosjean, D., 1992. In situ organic aerosol formation during a smog episode: Estimated production and chemical functionality. Atmos. Environ. Part A. Gen. Top. 26, 953–963. https://doi.org/https://doi.org/10.1016/0960-1686(92)90027-I

Hoffmann, T., Odum, J.A.Y.R., Bowman, F., Collins, D., Klockow, D., Flagan, R.C., Seinfeld, J.H., 1997. Formation of Organic Aerosols from the Oxidation of Biogenic Hydrocarbons. J. Atmos. Chem. 26, 189–222. https://doi.org/10.1023/A:1005734301837

Wang, C.-T., Wiedinmyer, C., Ashworth, K., Harley, P.C., Ortega, J., Vizuete, W., 2019. Leaf enclosure measurements for determining volatile organic compound emission capacity from Cannabis spp. Atmos. Environ. 199, 80–87. https://doi.org/https://doi.org/10.1016/j.atmosenv.2018.10.049

Yang, W., Zhang, B., Wu, Y., Liu, S., Kong, F., Li, L., 2023. Effects of soil drought and nitrogen deposition on BVOC emissions and their O(3) and SOA formation for Pinus thunbergii. Environ. Pollut. 316, 120693. https://doi.org/10.1016/j.envpol.2022.120693

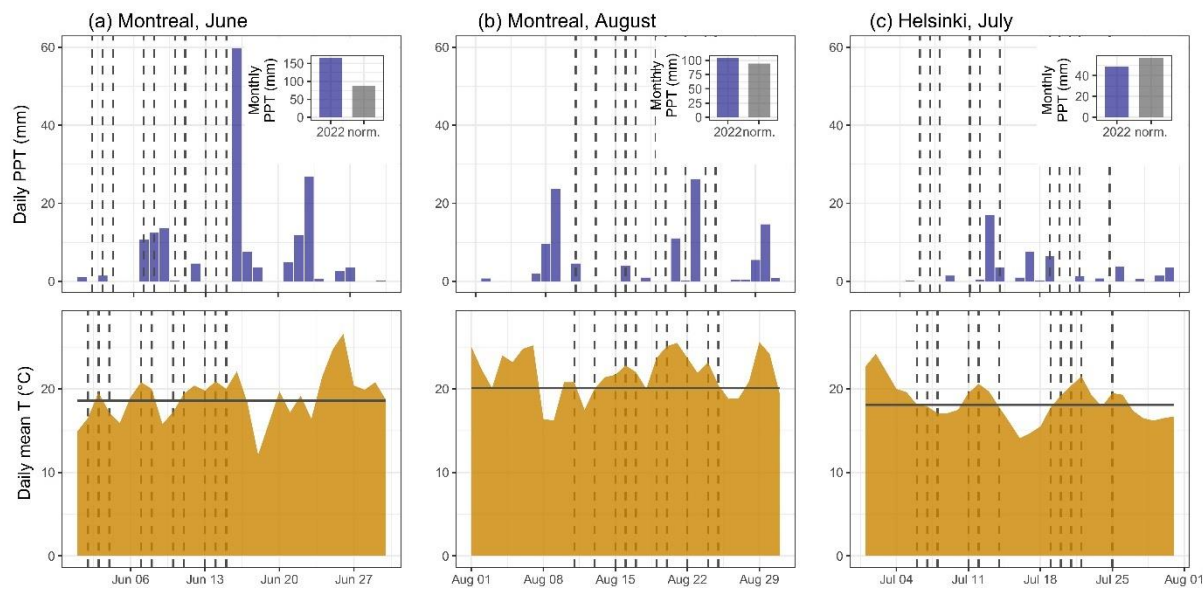


Figure S4. Daily precipitation totals (PPT) and daily mean temperatures (T) for (a) June and (b) August in Montreal, and (c) July in Helsinki, 2022. The vertical dashed lines indicate the sampling days during the measurement periods. In the precipitation figures, the monthly precipitation totals for 2022 and the precipitation normals are provided in inserts. In the temperature figure, the horizontal line indicates the normal mean temperature per month. The monthly climate normals for Montreal are reported for 1981–2010 (https://climat.meteo.gc.ca/) and in Helsinki for 1991–2020 (Jokinen et al. 2021).

https://climat.meteo.gc.ca/, last accessed 16.12.2024

Jokinen, P., Pirinen, P., Kaukoranta, J.-P., Kangas, A., Alenius, P., Eriksson, P., Johansson, M., Wilkman, S., 2021. Tilastoja Suomen ilmastosta 1991-2020. https://doi.org/https://doi.org/10.35614/isbn.9789523361485

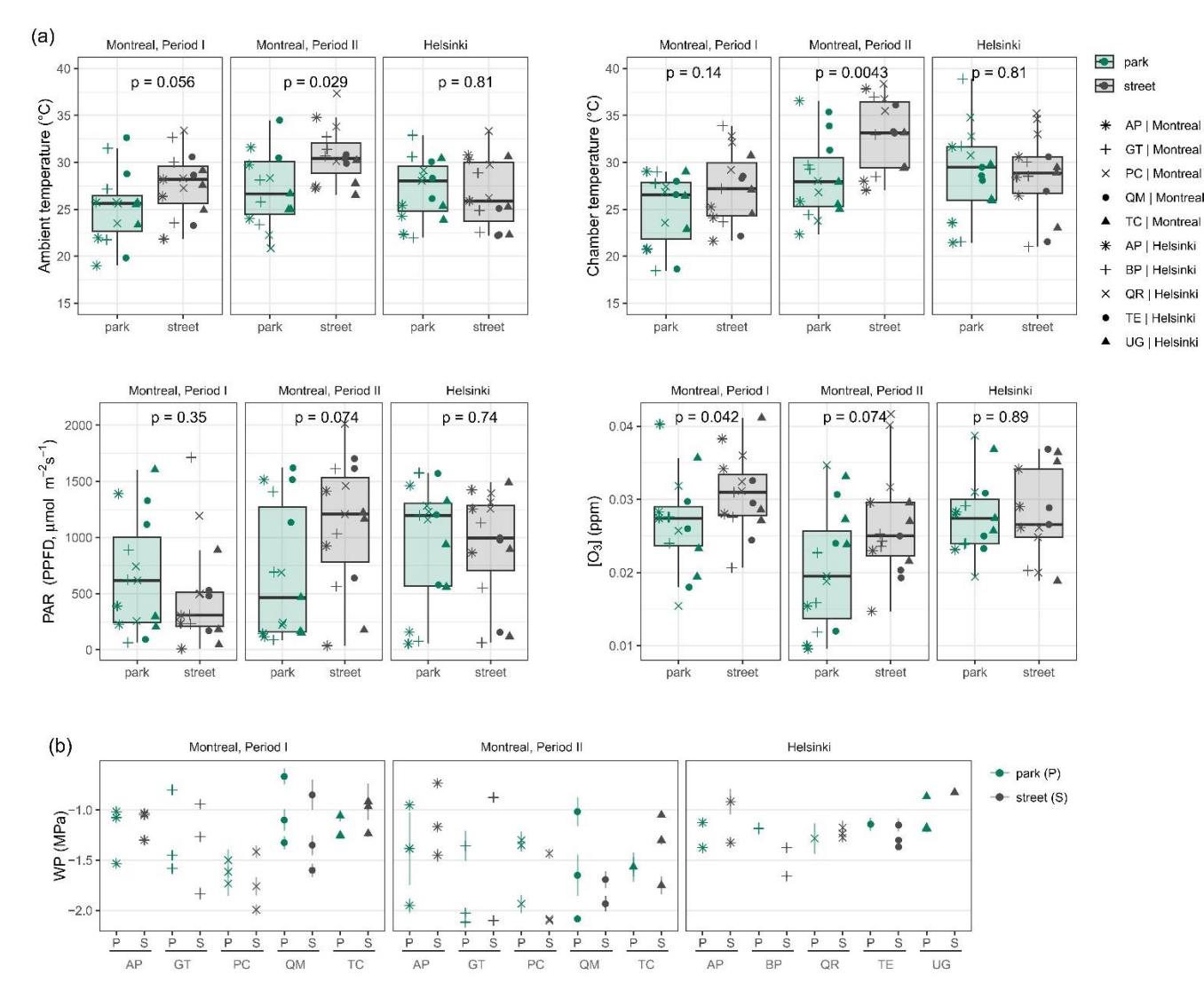


Figure S5. (a) Ambient and chamber temperatures, photosynthetically active radiation (PAR), and ambient O₃ concentrations during the sampling times separately for city, measurement period, and site type (street in black and park in green), and species (different shapes). The p-values are reported for the Wilcoxon tests between park and street conditions. (b) The mid-day leaf water potentials (WP) of the study trees after sampling, separately for city, measurement period, and site type, and per species. The error bars reflect 1 standard deviation. Species: AP, Acer platanoides; GT, Gleditsia triacanthos; PC, Populus canescens; QM, Quercus macrocarpa; TC, Tilia cordata; BP, Betula pendula; QR, Quercus robur; TE, Tilia x europaea; UG, Ulmus glabra.

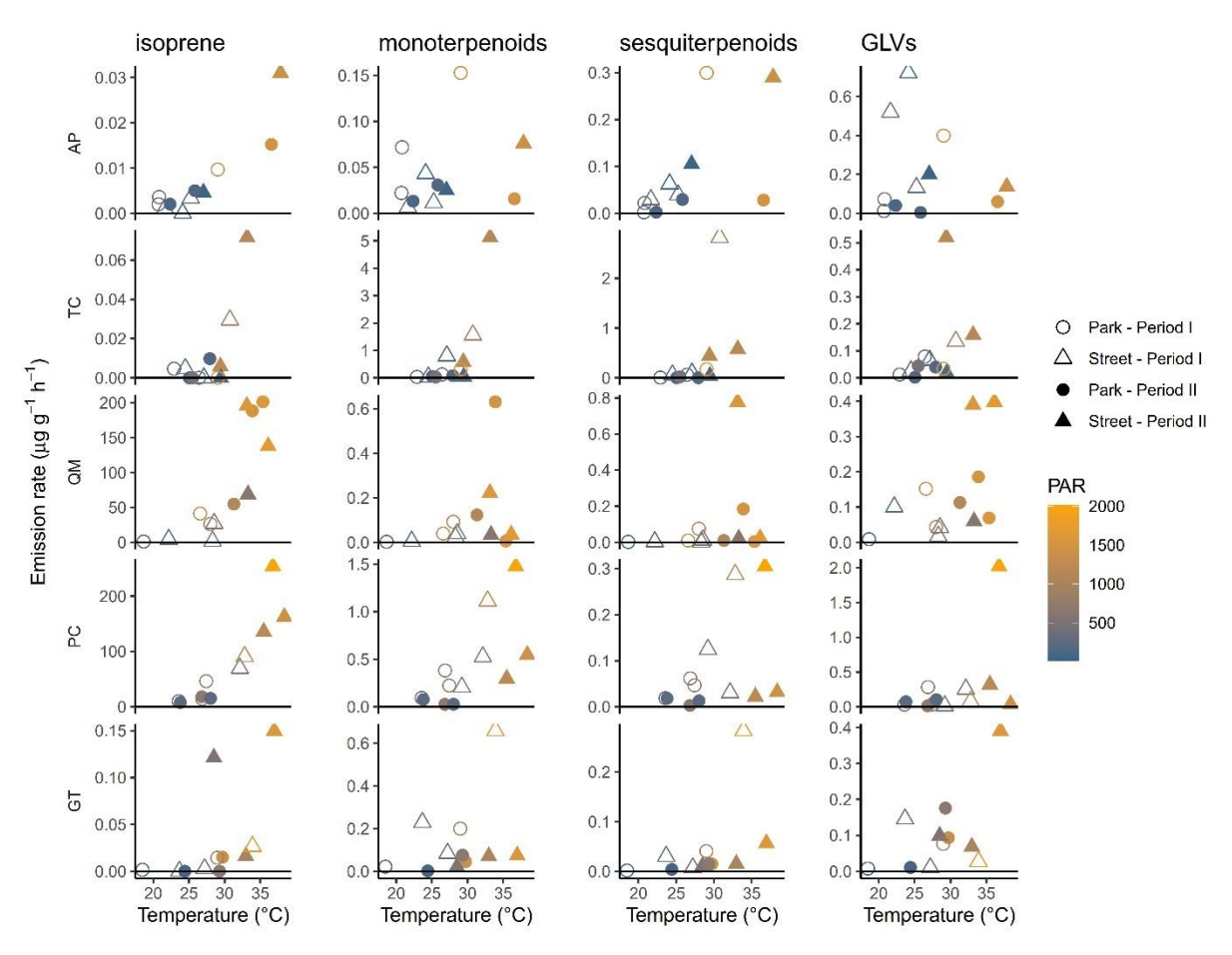


Figure S6. The emission rates of isoprene, and the monoterpenoid, sesquiterpenoid and green leaf volatile (GLV) totals for the study species (AP, Acer platanoides; GT, Gleditsia triacanthos; PC, Populus x canescens; QM, Quercus macrocarpa; TC, Tilia cordata) in parks (dots) and streets (triangles) in Montreal in July (period I, open symbols) and August (period II, filled symbols) in 2022, and in relation to enclosure temperature and photosynthetically active radiation (PAR) measured next to the enclosure (colour gradient).

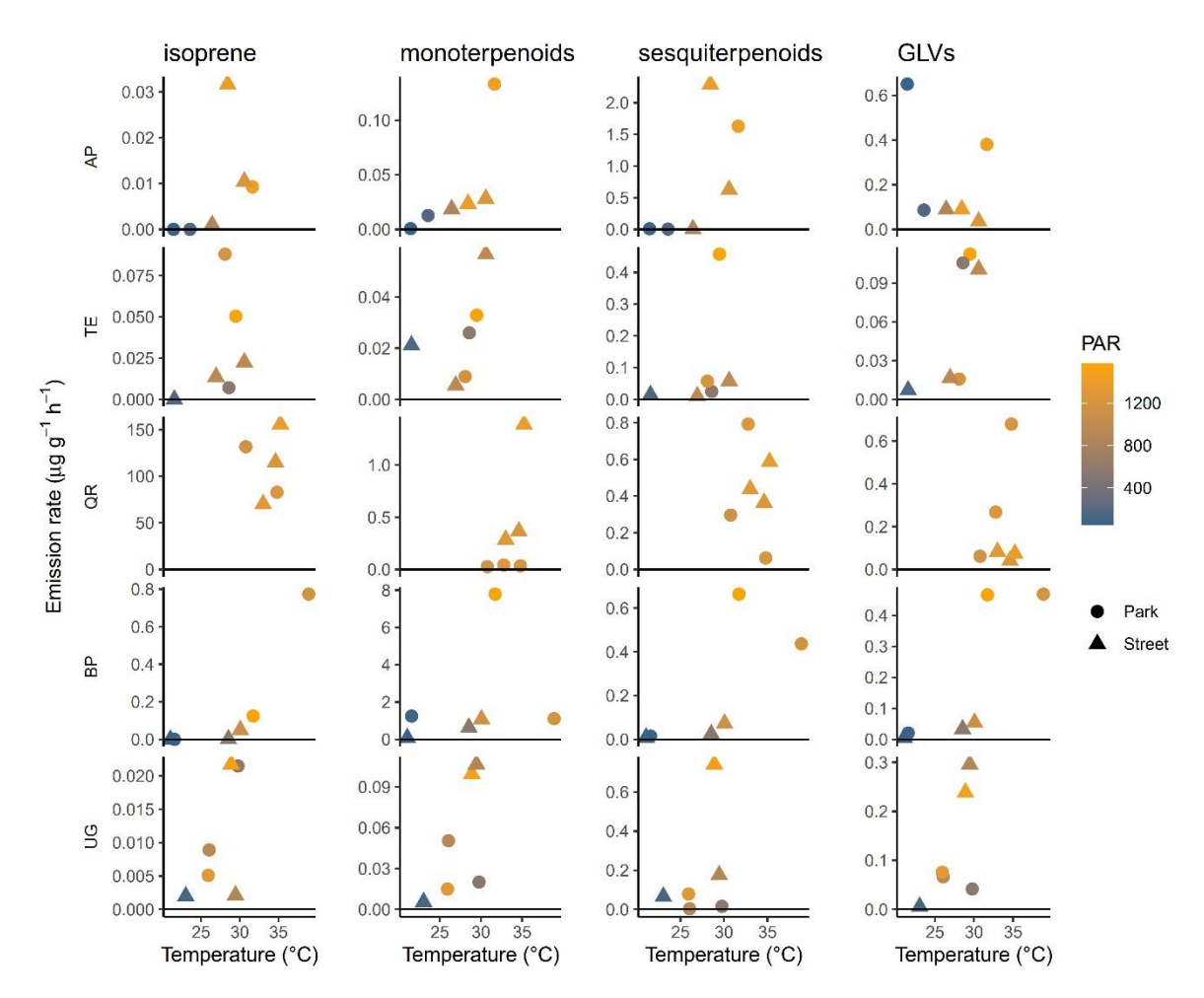


Figure S7. The emission rates of the isoprene, and the monoterpenoid, sesquiterpenoid and green leaf volatile (GLV) totals for the study species (AP, *Acer platanoides*; BP, *Betula pendula*; QR, *Quercus robur*; TE, *Tilia x europaea*; UG, *Ulmus glabra*) in parks (dots) and streets (triangles) in Helsinki in June 2022 in relation to the enclosure temperature and photosynthetically active radiation (PAR) measured next to the enclosure (colour gradient).

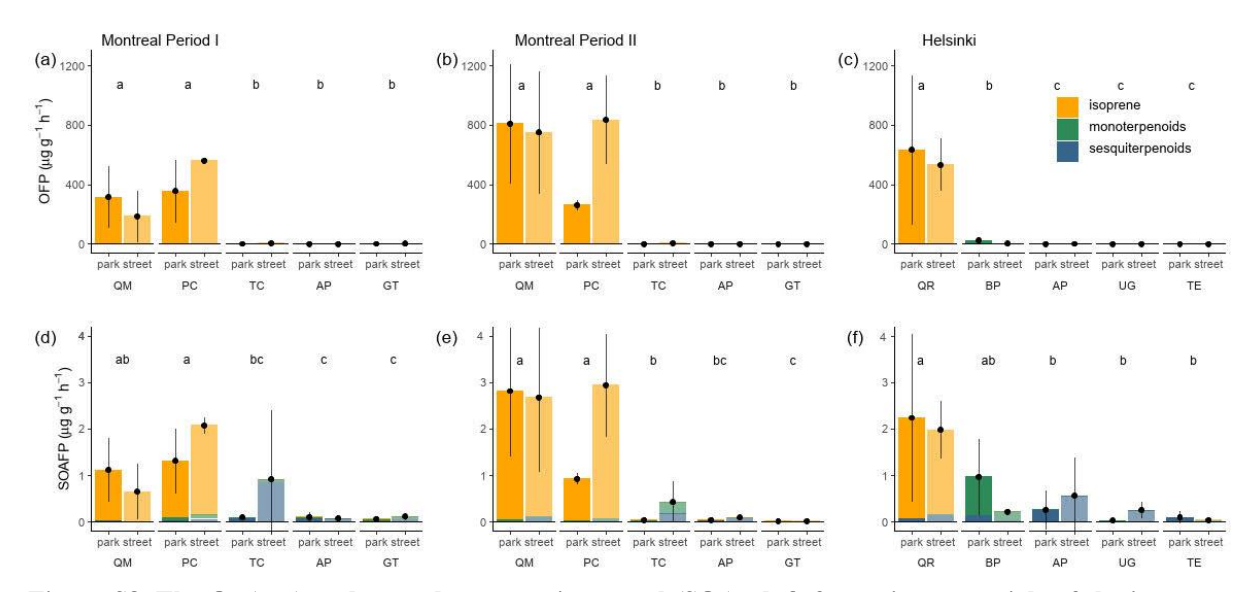


Figure S8. The O₃ (a–c) and secondary organic aerosol (SOA; d–f) formation potentials of the isoprene, monoterpenoid and sesquiterpenoid emissions by urban tree species and the measurement period studied in Montreal (a, b, d and e) and Helsinki (c and f). The dot with whiskers indicates the mean and 95% confidence intervals of the O₃- or SOA-formation potentials across the measured individuals of the species and the bars indicate the mean contribution of the isoprene, monoterpenoids, and sesquiterpenoids for the potentials. The different lowercase letters indicate a significant difference between species within the city and measurement period in Montreal. OFP or SOAFP were calculated from the BVOC emission potentials normalised using the median temperature for the sampling period (28°C in Montreal and 27°C in Helsinki). Species: AP, Acer platanoides; GT, Gleditsia triacanthos; PC, Populus canescens; QM, Quercus marcrocarpa; TC, Tilia cordata; BP, Betula pendula; QR, Quercus robur; TE, Tilia x europaea; UG, Ulmus glabra.